applied sciences

MDPI

*Communication*

# Synthesis of Proposed Structure of Aaptoline B via Transition Metal-Catalyzed Cycloisomerization and Evaluation of Its Neuroprotective Properties in *C. Elegans*

**Soobin Kim [1], Wooin Yang [2], Dong-Seok Cha [2,*] and Young-Taek Han [1,*]**

[1] College of Pharmacy, Dankook University, 119 Dandae-ro, Dongnam-gu, Cheonan-si 31116, Chungnam, Korea; rue42351@naver.com
[2] College of Pharmacy, Woosuk University, 443 Samnye-ro, Wanju-gun 55338, Jeonbuk, Korea; benefinn@naver.com
* Correspondence: hanyt@dankook.ac.kr (Y.-T.H.); cha@woosuk.ac.kr (D.-S.C.); Tel.: +82-41-550-1431 (Y.-T.H.)

**Abstract:** A concise synthesis of the proposed structure of aaptoline B, a pyrroloquinoline derived from a marine sponge, was accomplished. A key feature of this synthesis is the versatile transition metal-catalyzed cycloisomerization of *N*-propargylaniline to construct a quinoline skeleton. However, the spectral data of the synthesized aaptoline B did not agree with those of previous studies. The structure of the synthesized aaptoline B was confirmed using a combined 2D NMR analysis. Furthermore, we assessed the possible neuroprotective potential of aaptoline B using the *C. elegans* model system. In this study, aaptoline B significantly improved the viability and the morphology of dopaminergic neurons of nematodes under $MPP^+$ exposure conditions. We also found that $MPP^+$-induced motor deficits in nematodes were efficiently restored by aaptoline B treatment. Our findings demonstrate the neuroprotective effects of aaptoline B against $MPP^+$-induced dopaminergic neuronal damage. Further studies are underway to explain its pharmacological mechanism.

**Keywords:** aaptoline B; pyrroloquinoline; Ag(I)-catalyzed cycloisomerization; dopaminergic neuroprotection; Parkinson's disease

**Citation:** Kim, S.; Yang, W.; Cha, D.-S.; Han, Y.-T. Synthesis of Proposed Structure of Aaptoline B via Transition Metal-Catalyzed Cycloisomerization and Evaluation of Its Neuroprotective Properties in *C. Elegans*. *Appl. Sci.* **2021**, *11*, 9125. https://doi.org/10.3390/app11199125

Academic Editors: Ana M. L. Seca and Monica Gallo

Received: 13 September 2021
Accepted: 28 September 2021
Published: 30 September 2021



## 1. Introduction

Parkinson's disease (PD) is a progressive neurodegenerative disorder of the central nervous system that affects millions of people worldwide. The clinical features of PD include impaired motor functions and nonmotor symptoms, which are mainly due to the selective loss of dopaminergic neurons in the substantia nigra pars compacta (SNpc) [1]. Although the underlying pathological mechanism of PD remains unknown, overproduction of reactive oxygen species (ROS) is considered a major trigger of neuronal death in the SNpc [2]. In addition, neurotoxins such as 1-methyl-4-phenylpyridinium ($MPP^+$) and 6-hydroxydopamine (6-OHDA) can induce dopaminergic neurodegeneration via mitochondrial dysfunction and consequent ROS generation, and the treated animals exhibit symptoms similar to humans with PD [3].

Aaptoline B (**1**) has been reported as a pyrroloquinoline alkaloid isolated from the marine sponge *Aaptos aaptos* by a Chinese research group [4]. Structurally, as shown in Figure 1, **1** is characterized by a unique 7*H*-pyrrolo [2,3-h]quinoline skeleton embedded with privileged scaffolds, such as indole and quinoline. Indole and quinoline derivatives exhibit diverse biological activities, including anticancer and anti-neurodegenerative diseases. Hence, these two scaffolds, including their heterocycle-linked and fused analogs, have been considered important privileged scaffolds in drug discovery [5–7].

Recently, we have intensively worked on the synthesis and biological applications of pyridine-fused privileged scaffolds, such as quinoline and pyridocoumarin, using Ag(I)-

catalyzed cycloisomerization [8–10]. Taking advantage of its high yield and regioselectivity, Ag(I)-catalyzed cycloisomerization has also been used for the synthesis of natural products, including goniothalines [8] and polynemoraline C [10]. These successful results of the construction of pyridine-fused skeletons via Ag(I)-catalyzed cycloisomerization as well as interesting structural features of the pyrroloquinoline scaffold of **1** prompted us to attempt the total synthesis of **1**. This paper describes the total synthesis of the proposed structure of **1** and its protective properties against $MPP^+$-induced dopaminergic neurodegeneration using the *Caenorhabditis elegans* model, which offers an excellent environment for PD research.

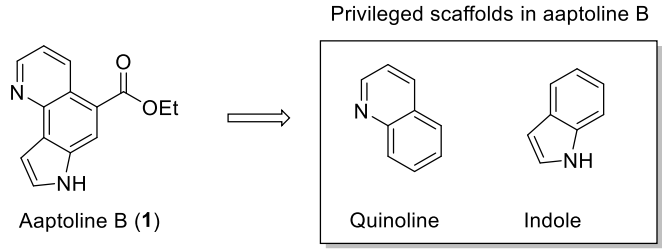


**Figure 1.** Proposed structure of pyrroloquinoline alkaloid aaptoline B (**1**) and embedded privileged scaffolds.

## 2. Materials and Methods

### *2.1. Chemistry*

#### 2.1.1. General Experimental

Unless otherwise noted, all reactions were performed under an argon atmosphere in oven-dried glassware. The starting materials and solvents were used as received from commercial suppliers without further purification. Thin layer chromatography was carried out using Merck silica gel 60 F254 plates, and visualized with a combination of UV, *p*-anisaldehyde, and potassium permanganate staining. Flash chromatography was performed using Merck silica gel 60 (0.040–0.063 mm, 230–400 mesh). Mass spectra were obtained using an Agilent 6530 Q-TOF unit. $^1$H and $^{13}$C spectra were recorded on a Bruker 500/54 Ascend (500 MHz) spectrometer at the Center for Bio-medical Engineering Core Facility (Dankook University, Korea), Jeol RESONANCE ECZ 400S (400 MHz), or Bruker Ascend III (700 MHz) in deuterated solvents. $^1$H and $^{13}$C NMR chemical shifts are reported in parts per million (ppm) relative to TMS, with the residual solvent peak used as an internal reference. Signals are reported as m (multiplet), s (singlet), d (doublet), t (triplet), q (quartet), bs (broad singlet), bd (broad doublet), dd (doublet of doublets), dt (doublet of triplets), or dq (doublet of quartets); the coupling constants are reported in hertz (Hz)

#### 2.1.2. Ethyl 4-methyl-3,5-dinitrobenzoate (**3**)

Ethyl benzoic acid **3** was obtained from **4** according to literature procedures with some modifications [11]. Briefly, to a solution of 3,5-dinitro-4-methylbenzoic acid (**4**; 3.00 g, 13.27 mmol) in 20 mL of anhydrous EtOH was slowly added 3 mL of $H_2SO_4$ at ambient temperature. After being refluxed overnight, the reaction mixture was cooled to ambient temperature, and concentrated in vacuo. Purification of residue via column chromatography on silica gel with $CH_2Cl_2$ afforded **3** (3.14 g, 93%) as a yellowish solid. The NMR spectra were consistent with the previously reported data. Melting point: 74~76 °C; $^1$H-NMR (500 MHz, $CDCl_3$) δ 8.59 (s, 2H), 4.46 (q, 2H, $J$ = 7.1 Hz), 2.63 (s, 3H), 1.43 (t, 3H, $J$ = 7.1 Hz); $^{13}$C-NMR (125 MHz, $CDCl_3$) δ 162.5, 151.6, 131.3, 130.6, 127.8, 62.7, 15.2, 14.2.

2.1.3. Ethyl 4-amino-1*H*-indole-6-carboxylate (**6**)

To a solution of **3** (300 mg, 1.18 mmol) in 0.3 mL of DMF was added *N*,*N*-dimethylformamide diethyl acetal (0.45 mL, 2.6 mmol) at ambient temperature. The reaction mixture was heated at 50 °C for 1 h, and concentrated in vacuo to give crude enamine **5**. To a solution of the residue in EtOH (60 mL) was added catalytic amount of 10% palladium on carbon. The reaction mixture was stirred under a hydrogen atmosphere until TLC analysis showed the complete disappearance of **5**, and filtered using a Celite pad. The filtrate was concentrated in vacuo. Purification of the residue via flash column chromatography (EtOAc:*n*-hexane = 1:1) afforded amino-1*H*-indole **6** (191 mg, 78% in 2 steps) as a dark-red gum. $^{1}$H-NMR (500 MHz, $CD_3OD$) δ 7.57 (s, 1H), 7.28 (s, 1H), 7.02 (s, 1H), 6.56 (s, 1H), 4.59 (s, 1H), 4.32 (d, 2H, *J* = 5.8 Hz), 1.38 (s, 3H); $^{13}$C-NMR (125 MHz, $CD_3OD$) δ 170.1, 140.8, 137.7, 127.0, 125.3, 123.2, 106.1, 105.0, 99.9, 61.6, 14.7; HR-MS (Q-ToF): Calcd for $C_{11}H_{13}N_2O_2^+$ (M + $H^+$): 205.0972. Found: 205.0977.

2.1.4. Ethyl 4-(prop-2-yn-1-ylamino)-1*H*-indole-6-carboxylate (**2**)

To a solution of **6** (30 mg, 0.147 mmol), KI (2.4 mg, 14.7 μmol) and $K_2CO_3$ (44.6 mg, 0.323 mmol) in DMF (1.5 mL) was added 24.1 mg (0.162 mmol) of 80 w/w% solution of propargyl bromide in toluene at ambient temperature. The reaction mixture was stirred for 72 h at 65 °C, cooled to ambient temperature, and then diluted with water and EtOAc. The organic layer was washed with water and brine, dried over $MgSO_4$, and concentrated in vacuo. Purification of residue via column chromatography on silica gel (EtOAc:*n*-hexane = 1:4~1:1) afforded *N*-propargyl aminobenzoate **2** (21.8 mg, 61%) as a dark-yellow oil along with 4.2 mg of starting material **6** (71% yield brsm). $^{1}$H-NMR (400 MHz, $CDCl_3$) δ 8.47 (s, 1H), 7.71 (d, 1H, *J* = 0.9 Hz), 7.25 (m, 2H), 7.09 (d, 1H, *J* = 0.9 Hz), 6.52 (m, 1H), 4.38 (q, 2H, *J* = 7.1 Hz), 4.15 (d, 2H, *J* = 2.5 Hz), 2.26 (t, 1H, *J* = 2.4 Hz), 1.40 (t, 3H, *J* = 7.1 Hz) ; $^{13}$C-NMR (100 MHz, $CDCl_3$) δ 167.4, 135.1, 125.0, 125.0, 120.5, 105.4, 100.9, 98.7, 80.1, 71.5, 60.2, 33.6, 14.0; HR-MS (Q-ToF): Calcd for $C_{14}H_{15}N_2O_2^+$ (M + $H^+$): 243.1128. Found: 243.1131.

2.1.5. Representative Procedure of Transition Metal-Catalyzed Cycloisomerization for Ethyl 7*H*-pyrrolo [2,3-h]quinoline-5-carboxylate (Aaptoline B; **1**)

To a solution of **2** (21.8 mg, 0.09 mmol) in DMSO (2.3 mL) was added $AgSbF_6$ (3.1 mg, 9 μmol) at ambient temperature. The reaction mixture was stirred at 110 °C for 4.5 h, cooled to ambient temperature, diluted with EtOAc and quenched with saturated aq. $NaHCO_3$ solution. The organic layer was washed with water and brine, dried over $Na_2SO_4$, and concentrated in vacuo. Purification of residue via column chromatography on silica gel (EtOAc:*n*-hexane = 1:3~1:1) afforded aaptoline B (**1**; 14.1 mg, 73%) as a yellowish solid. Melting point: 187~190 °C; $^{1}$H-NMR (500 MHz, $CDCl_3$) δ 9.56 (d, 1H, *J* = 8.4 Hz), 9.43 (s, 1H), 8.96 (d, 1H, *J* = 3.2 Hz), 8.52 (s, 1H), 7.52 (m, 3H), 4.47 (q, 2H, *J* = 7.1 Hz), 1.46 (t, 3H, *J* = 7.1 Hz); $^{13}$C-NMR (125 MHz, $CDCl_3$) δ 167.3, 148.2, 143.1, 136.3, 133.1, 127.1, 126.8, 122.9, 120.4, 120.1, 119.5, 104.0, 61.2, 14.6; $^{1}$H-NMR (700 MHz, $CD_3OD$) δ 9.52 (dd, 1H, *J* = 1.4, 8.4 Hz), 8.79 (dd, 1H, *J* = 1.8, 4.6 Hz), 8.51 (s, 1H), 7.59 (d, 1H, *J* = 2.8 Hz), 7.51 (dd, 1H, *J* = 4.6, 8.8 Hz), 7.34 (t, 1H, *J* = 1.4 Hz), 4.45 (q, 2H, *J* = 7.2 Hz), 1.46 (t, 3H, *J* = 7.0 Hz); $^{13}$C-NMR (175 MHz, $CD_3OD$) δ 168.7, 149.2, 144.7, 137.2, 134.7, 128.6, 128.2, 124.0, 121.1, 120.9, 120.8, 103.9, 62.2, 14.9; HR-MS (Q-ToF): Calcd for $C_{14}H_{13}N_2O_2^+$ (M + $H^+$): 241.0972. Found: 241.0977.

*2.2. Biology*

2.2.1. *C. Elegans* Maintenance and $MPP^+$ Treatment

Wild-type Bristol N2 and transgenic strain: BZ555 (egIs1, Pdat-1::GFP) were provided from the Caenorhabditis Genetic Center (CGC; University of Minnesota, Minneapolis, MN). Nematodes were maintained in the liquid medium with live *Escherichia coli*

bacteria (OP50) at 20 °C. After embryo isolation, age-synchronized young-adult nematodes were treated with **1** or vehicle for 2 h. Then the nematodes were incubated another 96 h under 4 mM of $MPP^+$ exposure.

#### 2.2.2. Fluorescence Microscopy and Visualization

On the 4th day of adulthood, 10% sodium azide was applied to nematodes and immobilized nematodes were transferred onto 2% agarose pad. The DA neuronal viability of the nematodes was evaluated by using a fluorescence microscope (Nikon Eclipse Ni-u, Japan). The GFP fluorescence signals of each animal were photographed and calculated the number of intact DA neurons.

#### 2.2.3. Behavioral Assay

Age-synchronized N2 nematodes were incubated with or without **1**. On the 4th day of adulthood, their motor abilities were observed using a dissecting microscope (Nikon SMZ1500, Japan) and Nikon image analysis software 4.0(NIS-Elements, Japan). The travel distance of nematodes was automatically recorded for 20 s. For the food sensing assay, nematodes were washed with M9 buffer 3 times to remove any residual food and then transferred to a nonfood plate. The velocity of nematodes on the nonfood plate was measured and then the velocity was measured again on the food plate.

#### 2.2.4. Statistical Analysis

All experiments were independently conducted at least thrice. The results were shown in mean ± S.D. Statistical significance of differences between groups were compared with one-way analysis of variance (ANOVA) followed by Tukey test.

## 3. Results and Discussion

### *3.1. Synthesis and Structure Elucidation of Aaptoline B*

The retrosynthetic analysis for **1** is depicted in Figure 2, which includes the 6-endo selective transition metal-catalyzed cycloisomerization of 4-propargylaminoindole **2**. Precursor **2** was expected to be readily synthesized from the known dinitrobenzoate **3** by Batcho–Leimgruber indole synthesis, a powerful synthetic method for the synthesis of indoles from ortho-nitrotoluenes, which proceeds via the formation of the enamine intermediates and subsequent reductive cyclization [12], followed by regioselective *N*-propargylation.

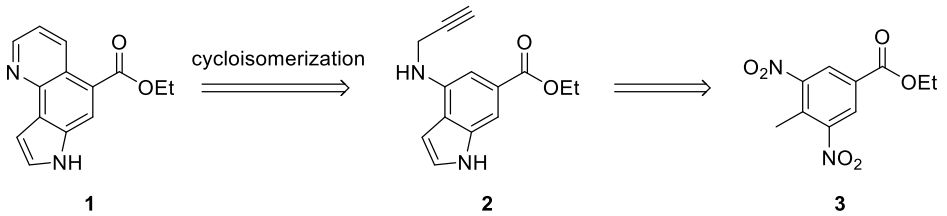


**Figure 2.** Retrosynthetic analysis of aaptoline B (**1**).

As shown in Scheme 1, our synthesis commenced with the preparation of previously reported ethyl 4-methyl-3,5-dinitrobenzoate **3**. Thus, benzoic acid **4** was refluxed in anhydrous ethyl alcohol in the presence of sulfuric acid to afford ethyl benzoate **3** [11]. When *N*,*N*-dimethylformamide dimethyl acetal was used, according to the literature [13] to obtain enamine **5** from **3**, followed by reductive cyclization, the indole ethyl carboxylate **6** was obtained as a mixture with the corresponding methyl ester **6′**. We supposed that methoxide or methanol, possibly generated from dimethylformamide dimethyl acetal, led to unexpected transesterification. Hence, we performed the Batcho–Leimgruber indole synthesis reaction of **3** using *N*,*N*-dimethylformamide diethyl acetal instead of dimethyl

acetal, and obtained ethyl indole carboxylate **6** in 74% (two steps from **3**) without methyl ester byproducts. To minimize side reactions, such as over-alkylation and *N*-alkylation of pyrrolic nitrogen atom, we intensively investigated the reaction conditions of *N*-propargylation of **6** into 4-propargylaminoindole **2** by altering the amount of reagents, reaction time, and temperature. The optimal yield (61% isolated yield; 71% brsm yield) was achieved without *N*-alkylation of aromatic pyrrolic amine when the DMF solution of **2** and 1.1 equivalents of propargyl bromide was heated at 65 °C for 72 h with 2.2 equivalents of $K_2CO_3$ and a catalytic amount of KI [14].

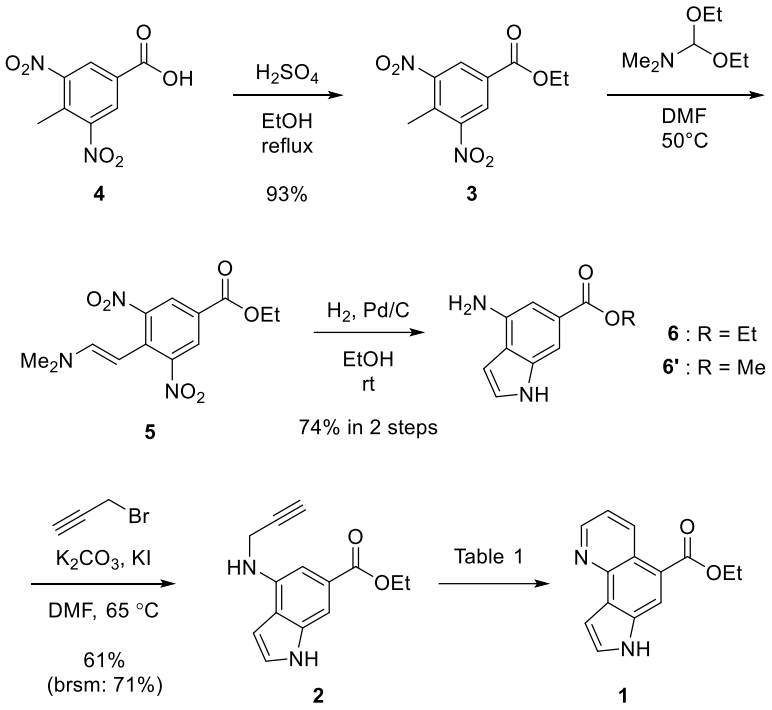


**Scheme 1.** Synthesis of proposed structure of aaptoline B (**1**).

With the cycloisomerization precursor **2** in hand, we tested diverse transition metal catalysts (Table 1) to find out the optimal reaction conditions. We initially carried out cycloisomerization of **2** with 0.1 equivalent of CuI (entry 1), and obtained **1** with 56% yield. When the reaction was conducted with $InCl_3$ (entry 2) or AuCl (entry 3), the yields (18% and 27%, respectively) were poorer. The use of $AgSbF_6$ as catalyst resulted in the best yield (73%, entry 4), being superior to other catalysts of Ag(I), such as $AgNO_3$ (61%; entry 5) and AgOTf (35%; entry 6).

**Table 1.** Catalyst screening for the completion of synthesis of proposed structure of **1**.

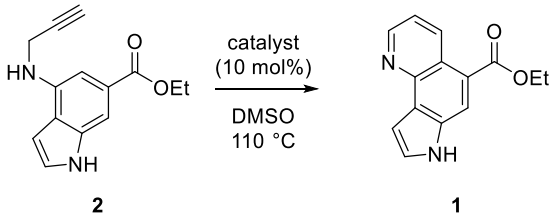


| Entry [1] | Catalyst | Time (h) | Yield [2] (%) |
|---|---|---|---|
| 1 | CuI | 2 | 56 |
| 2 | $InCl_3$ | 27 | 18 |
| 3 | AuCl | 8 | 27 |
| 4 | $AgSbF_6$ | 4.5 | 73 |

| | | | |
|---|---|---|---|
| 5 | $AgNO_3$ | 5 | 61 |
| 6 | AgOTf | 5 | 35 |

[1] 30 mg of **7** in DMSO (0.1 M solution) was reacted; [2] Isolated yields.

However, the NMR spectra of **1** differed from those reported when using the same deuterated solvent ($CDCl_3$). Significant differences were observed in both the $^1H$ and $^{13}C$ NMR spectra of our synthetic sample compared to those of the isolated product [4]. To precisely confirm the structure of synthetic **1**, we employed two-dimensional NMR analysis (700 MHz, $CD_3OD$; see the Supplementary Materials). Proton at C-3 was clearly revealed by homonuclear correlation spectroscopy ($^1H$-$^1H$ COSY) by correlations with the neighboring aromatic protons on C-2 and C-4, which were confirmed by further investigation employing heteronuclear correlation spectroscopy. Singlet peak at 8.51 ppm ($^1H$ NMR in $CD_3OD$) did not exhibit any correlation in $^1H$-$^1H$ COSY, and it was confirmed as proton at C-6. The $^{13}C$-NMR peaks of all hydrogenated carbons could be assigned unambiguously based on heteronuclear single quantum coherence ($^1H$-$^{13}C$ HSQC) analysis. The $^{13}C$-NMR peaks of the quaternary carbons (5 and 7–12) were carefully assigned using the HMBC correlation. Because it was difficult to find a significant difference in HMBC correlations from their neighboring carbons, C-9~12 were hard to be confirmed using 2D NMR analysis. For instance, C-9 and C-10 at the quinoline moiety exhibited the same HMBC correlation with neighboring protons.

Taking into consideration the previous assignments of $^1H$-NMR of the indole system [15], protons at δ 7.34 and δ 7.59 were assigned as protons on C-11 and C-12, respectively. Furthermore, based on preceding literature in which the peaks observed at about 125 and 145 ppm were designated as C-9 and C-10 carbon adjacent to nitrogen atom, respectively [16–18], the peak at δ 144.7 was assigned as carbons at C-10. Through two-dimensional NMR analysis, we were also able to assign the $^{13}C$-NMR peak of C-9 (δ 120.8) that could not be assigned in the previous study [4]. Overall, our assignment of **1** seems to be more reasonable compared to the previous report. The selected HMBC correlations are shown in Figure 3.

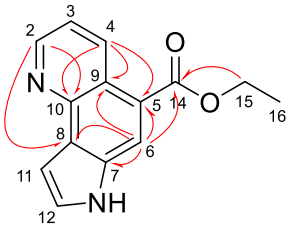


**Figure 3.** Selected HMBC correlations (H→C) of synthesized **1**.

*3.2. Evaluation of Neuroprotective Potential of Aaptoline B*

The neuroprotective potential of aaptoline B (**1**) was investigated using a *C. elegans* PD model. To test the effect of **1** on dopaminergic neuronal loss induced by $MPP^+$, we analyzed the fluorescent signals of the transgenic nematode BZ555 (Pdat-1::GFP), which expresses GFP in dopaminergic neurons. As shown in Figure 4A,B, the treatment of nematodes with $MPP^+$ for 96 h significantly decreased the viability of neurons to 46.3 ± 5.6%. Compared to untreated nematodes, **1**-fed nematodes exhibited a notable increase in GFP signals of all eight dopaminergic neurons in a dose-dependent manner (Figure 4A,B). These findings indicate that **1** might have the ability to protect dopaminergic neurons against $MPP^+$-induced neurotoxicity. To confirm the protective role of **1** in the $MPP^+$-mediated dopaminergic neuronal damage, we examined whether **1** could modulate behaviors requiring dopamine function, such as food-sensing response and locomotion. Well-fed nematodes reduce their movement in the presence of food as compared to that af-

forded in its absence. This basal slowing response is known to be mediated solely by dopaminergic neural circuitry. In the current study, normal nematodes demonstrated a 73.5% reduction in locomotory velocity when they came across the bacterial lawn (Figure 4C). When the nematodes were exposed to $MPP^+$, the slowing response was significantly decreased to 37.2%, and treatment with **1** efficiently restored this reduction in the slowing response induced by $MPP^+$ (Figure 4C). In addition, we observed the effect of **1** on the travel distance of nematodes under $MPP^+$ exposure conditions. Similar to the results from the food-sensing assay, the travel distance of nematodes was significantly decreased in the presence of $MPP^+$, while **1** supplementation restored these $MPP^+$-induced defects in motor activities of nematodes in a dose-dependent manner (26.0%, 35.5%, and 38.2% at 5, 10, and 20 μM, respectively) (Figure 4D). Overall, our findings indicate that **1** could contribute to ameliorating dopaminergic neurodegeneration not only morphologically but also functionally.

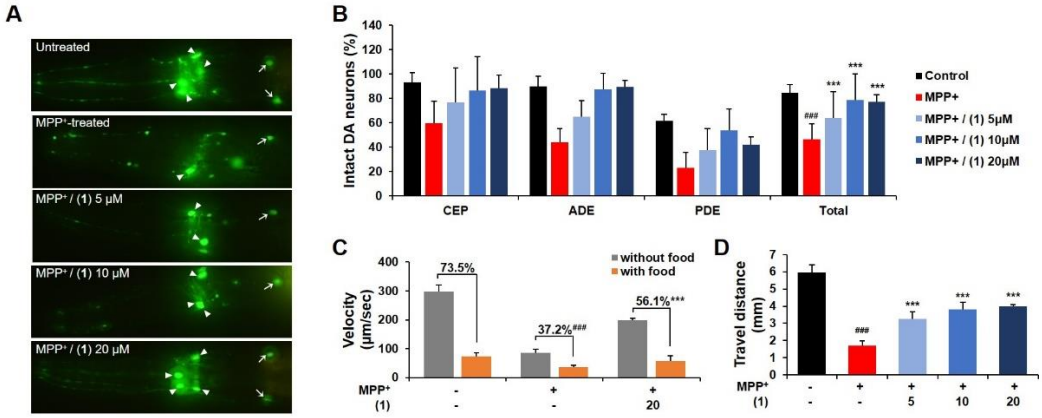


**Figure 4.** Neuroprotective effects of synthesized **1** on the DA neurodegeneration in the $MPP^+$-exposed *C. elegans*. (**A**) GFP fluorescence signals of CEP (arrowhead) and ADE (arrow) in the Pdat-1::GFP nematode were photographed at 400× magnification. (**B**) The viability of all eight DA neurons was scored by inspecting the GFP expressions of Pdat-1::GFP nematode. (**C**) The velocity of wild-type nematodes was observed in the presence or absence of food (*E. coli* OP50) and the basal slowing response was calculated. (**D**) The travel distance of wild-type nematodes was recorded for 20 s under a dissecting microscope. Statistical significance was determined by one-way ANOVA; $^{###}$ $p < 0.001$ compared with vehicle alone; *** $p < 0.001$ compared with $MPP^+$-treated control.

## 4. Conclusions

In summary, a concise and efficient synthesis of the proposed structure of aaptoline B was accomplished. Key features of the synthesis involve Batcho–Leimgruber indole synthesis and subsequent $AgSbF_6$-catalyzed cycloisomerization for the construction of the unique pyrrolo [2,3-h]quinoline skeleton of **1**. The spectral data of synthesized **1** did not agree with those in a previous report. However, the structure of the synthesized ethyl 7*H*-pyrrolo [2,3-h]quinoline-5-carboxylate (**1**), originally proposed as aaptoline B, was confirmed using combined two-dimensional NMR analysis. Our findings from a biological study revealed that **1** could protect *C. elegans* from $MPP^+$-induced dopaminergic neuronal damage and restore dopamine-related behavioral functions, suggesting its therapeutic potential in PD. Further studies, such as pharmacophore identification and structure modification of **1**, were currently underway.

**Supplementary Materials:** The following are available online at www.mdpi.com/article/10.3390/app11199125/s1, Table S1: $^1H$- and $^{13}C$-NMR assignment of aaptoline B.

**Author Contributions:** Y.-T.H. and D.-S.C. conceived and designed the experiments, and wrote the paper; S.K. performed the synthesis and chemical analysis; W.Y. performed biological studies. All authors have read and agreed to the published version of the manuscript.

**Funding:** This research was funded by National Research Foundation of Korea (NRF-2020R1F1A1058295).

**Institutional Review Board Statement:** Not applicable.

**Informed Consent Statement:** Not applicable.

**Data Availability Statement:** Not applicable.

**Acknowledgments:** The authors gratefully acknowledge Center for Bio-Medical Engineering Core Facility for providing analytical equipment of Dankook University.

**Conflicts of Interest:** The authors declare no conflict of interest.

## References

1. Sveinbjornsdottir, S. The clinical symptoms of Parkinson's disease. *J. Neurochem.* **2016**, *139*, 318–324.
2. Mosley, R.L.; Benner, E.J.; Kadiu, I.; Thomas, M.; Boska, M.D.; Hasan, K.; Laurie, C.; Gendelman, H.E. Neuroinflammation, oxidative stress and the pathogenesis of Parkinson's disease. *Clin. Neurosci. Res*. **2006**, *6*, 261–281.
3. Nass, R.; Hall, D.H.; Miller, D.M.; Blakely, R.D. Neurotoxin-induced degeneration of dopamine neurons in *Caenorhabditis elegans*. *Proc. Natl. Acad. Sci. USA* **2002**, *99*, 3264–3269.
4. Tang, W.Z.; Yu, H.B.; Lu, J.R.; Lin, H.W.; Sun, F.; Wang, S.P.; Yang, F. Aaptolines A and B, two new quinoline alkaloids from the marine sponge *Aaptos aaptos*. *Chem. Biodivers.* **2020**, *17*, e2000074.
5. de Sá Alves, F.R.; Barreiro, E.J.; Fraga, C.A. From nature to drug discovery: The indole scaffold as a 'privileged structure'. *Mini-Rev. Med. Chem.* **2009**, *9*, 782–793.
6. Bongarzone, S.; Bolognesi, M.L. The concept of privileged structures in rational drug design: Focus on acridine and quinoline scaffolds in neurodegenerative and protozoan diseases. *Expert Opin. Drug Discov.* **2011**, *6*, 251–268.
7. Musiol, R. An overview of quinoline as a privileged scaffold in cancer drug discovery. *Expert Opin. Drug Discov.* **2017**, *12*, 583–597.
8. Ahn, S.; Yoon, J.A.; Han, Y.T. Total synthesis of the natural pyridocoumarins goniothaline A and B. *Synthesis* **2019**, *51*, 552–556.
9. Yoon, J.A.; Lim, C.; Han, Y.T. Preliminary study on novel expedient synthesis of 5-azaisocoumarins by transition metal-catalyzed cycloisomerization. *Front. Chem.* **2020**, *8*, 772.
10. Yoon, J.A.; Han, Y.T. Efficient synthesis of pyrido [3, 2-c] coumarins via silver nitrate catalyzed cycloisomerization and application to the first synthesis of polyneomarline C. *Synthesis* **2019**, *51*, 4611–4618.
11. Pickaert, G.; Ziessel, R. Synthesis of oligopyridinic scaffolds from amido substituted phenyl rings for extended hydrogen bonding. *Synthesis* **2004**, 2716–2726.
12. Li, J.J. *Name Reactions in Heterocyclic Chemistry*; John Wiley & Sons: Hoboken, NJ, USA, 2005; pp. 104–109.
13. Demont, H.E.; Faller, A.; MacPherson, D.T.; Milner, P.H.; Naylor, A.; Redshaw, S.; Stanway, S.J.; Vesey, R.D.; Walter, D.S. Preparation of Hydroxyethylamine Derivatives for the Treatment of Alzheimer's Disease. WO 2004050619A1, 17 June 2004.
14. Zhao, Y.; Cai, L.; Huang, T.; Meng, S.; Chan, A.S.; Zhao, J. Solvent-mediated C3/C7 regioselective switch in chiral phosphoric acid-catalyzed enantioselective Friedel-Crafts alkylation of indoles with $\alpha$-ketiminoesters. *Adv. Synth. Catal.* **2020**, *362*, 1309–1316.
15. Joule, J.A. *Product Class 13: Indole and Its Derivatives*; Thieme: Stuttgart, Germany, 2001; Volume 10, pp. 361–652.
16. da Rosa Monte Machado, G.; Diedrich, D.; Ruaro, T.C.; Zimmer, A.R.; Lettieri Teixeira, M.; de Oliveira, L.F.; Jean, M.; Van de Weghe, P.; de Andrade, S.F.; Baggio Gnoatto, S.C.; et al. Quinolines derivatives as promising new antifungal candidates for the treatment of candidiasis and dermatophytosis. *Braz. J. Microbiol.* **2020**, *51*, 1691–1701.
17. Lloyd, L.S.; Adams, R.W.; Bernstein, M.; Coombes, S.; Duckett, S.B.; Green, G.G.; Lewis, R.J.; Mewis, R.E.; Sleigh, C.J. Utilization of SABRE-derived hyperpolarization to detect low-concentration analytes via 1D and 2D NMR methods. *J. Am. Chem. Soc.* **2012**, *134*, 12904–12907.
18. Krzymiński, K.; Malecha, P.; Zadykowicz, B.; Wróblewska, A.; Błażejowski, J. $^{1}$H and $^{13}$C NMR spectra, structure and physicochemical features of phenyl acridine-9-carboxylates and 10-methyl-9-(phenoxycarbonyl)acridinium trifluoromethanesulphonates–alkyl substituted in the phenyl fragment. *Spectrochim. Acta A Mol. Biomol. Spectrosc.* **2012**, *78*, 401–409.